Development of ASTRI high-temperature solar receivers

Joe Coventry, Maziar Arjomandi, Charles-Alexis Asselineau, Alfonso Chinnici, Clotilde Corsi, Dominic Davis, Jin-Soo Kim, Apurv Kumar, Wojciech Lipiński, William Logie, Graham Nathan, John Pye, and Woei Saw

Citation: AIP Conference Proceedings **1850**, 030011 (2017); doi: 10.1063/1.4984354
View online: http://dx.doi.org/10.1063/1.4984354
View Table of Contents: http://aip.scitation.org/toc/apc/1850/1
Published by the American Institute of Physics

Development of ASTRI High-Temperature Solar Receivers

Joe Coventry[1,a)], Maziar Arjomandi[2], Charles-Alexis Asselineau[1], Alfonso Chinnici[2], Clotilde Corsi[3], Dominic Davis[2], Jin-Soo Kim[3], Apurv Kumar[1], Wojciech Lipiński[1], William Logie[1], Graham Nathan[2], John Pye[1] and Woei Saw[2]

[1]*Research School of Engineering, Australian National University, Canberra, Australia*
[2] *School of Mechanical Engineering, University of Adelaide, Adelaide, South Australia 5005, Australia*
[3] *CSIRO Energy, Newcastle, NSW 2300, Australia*

[a)]Corresponding author: joe.coventry@anu.edu.au

Abstract. Three high-temperature solar receiver design concepts are being evaluated as part of the Australian Solar Thermal Research Initiative (ASTRI): a flux-optimised sodium receiver, a falling particle receiver, and an expanding-vortex particle receiver. Preliminary results from performance modelling of each concept are presented. For the falling particle receiver, it is shown how particle size and flow rate have a significant influence on absorptance. For the vortex receiver, methods to reduce particle deposition on the window and increase particle residence time are discussed. For the sodium receiver, the methodology for geometry optimisation is discussed, as well as practical constraints relating to containment materials.

INTRODUCTION

Three high-temperature solar receiver design concepts are being evaluated as part of the Australian Solar Thermal Research Initiative (ASTRI): a flux-optimised sodium receiver, a falling particle receiver, and an expanding-vortex particle receiver. ASTRI is an eight-year research program with participation by six Australian universities and the CSIRO, and the collaboration of several USA national laboratories and universities. It has the technical goal of lowering the levelised cost of electricity (LCOE) of concentrating solar thermal (CST) technologies in Australia to 0.12 AUD/kWh by 2020. The receiver technologies under development form part of a set of integrated plant configurations, with the receiver designed to operate under high-flux (~2 MW/m^2) and to achieve high efficiency with outlet temperatures in the range 650–850°C. The design requirements for each of the solar receiver concepts are intrinsically linked to the plant configuration. Each configuration has a 25 MWe s-CO_2 Brayton cycle for the power block, which sets the parameters of inlet and outlet temperature of the receivers.

FALLING PARTICLE RECEIVER

Solid particle receivers were first tested in the early 1980's[1]. After a long period with little development, other than some theoretical and modeling studies, the concept is finding renewed interest in recent years[2-5]. Research on the falling particle receiver led by the CSIRO has focused on heat transfer model development for a particle curtain[6], development of the concept for a commercial-scale system, and initial simplified performance analysis. Preliminary studies were done for a simple free falling particle receiver concept to investigate its design boundary and performance as a reference system[7]. Additional studies employing a new falling particle concept with improved performance are also being carried out, but are beyond the scope of this paper.

SolarPACES 2016
AIP Conf. Proc. 1850, 030011-1–030011-9; doi: 10.1063/1.4984354
Published by AIP Publishing. 978-0-7354-1522-5/$30.00

Heat Transfer Model

Solar radiation incident on the falling particle receiver is absorbed, scattered and transmitted through the particle curtain, then reflected back by the wall located behind the curtain. The reflected radiation again undergoes absorption and scattering to be finally transmitted across the curtain and out of the receiver. A Monte-Carlo (MC) ray tracing method was used to describe the radiation characteristics of the particle curtain formed during the particle fall. The MC code determined in detail the absorption and scattering phenomenon occurring in the discretised particle curtain. The particle volume fraction, which is essential for the MC ray tracing, is obtained numerically using CFD[8] (the Eulerian-Eulerian granular model) or analytically (by assuming no drag falling) where a simpler estimation is required. Particle size and properties used in this study are listed in Table 1. The calculation method for radiation characteristics of falling particles were validated with the experimental results[7, 9]

TABLE 1. Particle size and properties [9] considered for the falling particle receiver

Mass flow rate	~ 30 kg/s
Particle diameter	280 and 697μm
Packed particle reflectivity	0.09
Heat capacity	$365T^{0.18}$ J/kg K
Particle density	3,300 kg/m^3

Design Concept

The design requirements, listed in Table 2, were determined based on the overall ASTRI plant configuration. The receiver concept consists of 4 cavities, each spanning a 90° section of a surround solar field (Fig. 1).

TABLE 2. Design requirement and receiver configuration.

Design requirement	**Receiver configuration**
• Targeted outlet temperature: 800°C • Particle temperature difference: 147°C • Estimated total flow rate: 765 kg/s (average C_p=1.2 kJ/kg K) • Plant location: Alice springs, Australia • Reference capacity: 25 MW_e + 4 hrs storage	• Type: Multiple cavity (for surround field) • Number of cavities: 4 • Diameter of each cavity aperture: 6 m • Number of falling particle curtain per cavity: 3 • Width of falling particle curtain: 2.5 m • Effective height of falling particle curtain: 6 m • Average flow rate per falling width in design condition: 25.5 kg/s-m

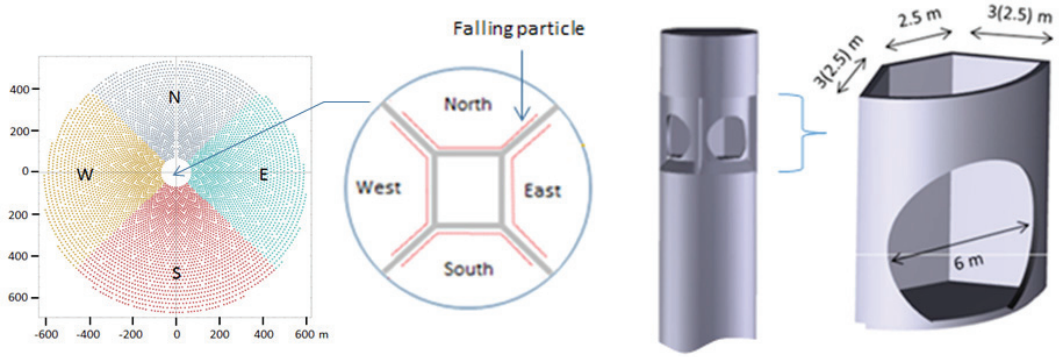

FIGURE 1. Concept geometry of a receiver employing 4 cavities compatible with the ASTRI reference field optimised for a system in Alice Springs, Australia, (assumed heliostat size: 6.1 m x 6.1 m, number of heliostats: 6,177, tower height: 92 m).

Performance Analysis

Using the heat transfer model for estimating solar energy absorption by the falling particle curtain, the overall solar energy absorptivity of a 6m high falling particle curtain was calculated for different flow rates and particle sizes. Considering the overall design capacity and the uneven solar input into the four cavities, the highest full load

particle flow rate per falling width was estimated to be 30 kg/s-m, which is deemed to be the flow rate of the southern cavity at solar noon on the equinox. The calculated absorptance is plotted in Fig. 2. The absorptance remains high in the high flow rate region but drops down rapidly when the flow rate is smaller than 10 kg/s-m. This means that a particle receiver with a smaller flow (e.g. high level of part load operation or a receiver designed for a larger temperature difference) will have a serious problem of low solar energy absorption due to increased transmission caused by the low volume fraction. In addition, the absorptance is highly affected by the particle size. As shown in Fig. 2, the 280 μm particle size showed higher solar energy absorptance and a much wider flow rate range with higher absorptance than the 697 μm case. A simplistic estimation of receiver performance was carried out by considering assumptions for different heat losses, as follows:

- Reflection and transmission energy loss: as per the absorptivity shown in Fig. 2a and multiplied by the ratio of aperture area to receiver surface area
- Emission heat loss: emission to surroundings at ambient temperature from an aperture size surface with 0.85 effective emissivity and 800°C temperature
- Convection heat loss: assumed to be 50 % of emission heat loss (estimated maximum convection heat loss using a simplified correlation by Kim et al.[10] at wind speed up to 6 m/s)

The estimated receiver performance is shown in Fig. 2b. Under full load design conditions, the receiver performance was 89.6% and 88.8% for 280 μm and 679 μm particle sizes, respectively. Under part load receiver operation with fixed inlet and outlet temperatures, receiver efficiency decreases as percentage load decreases. For a particle receiver, the efficiency decrease in part load operation is further enhanced by transmitted solar energy, which increases as the flow rate decreases and as the particle size increases.

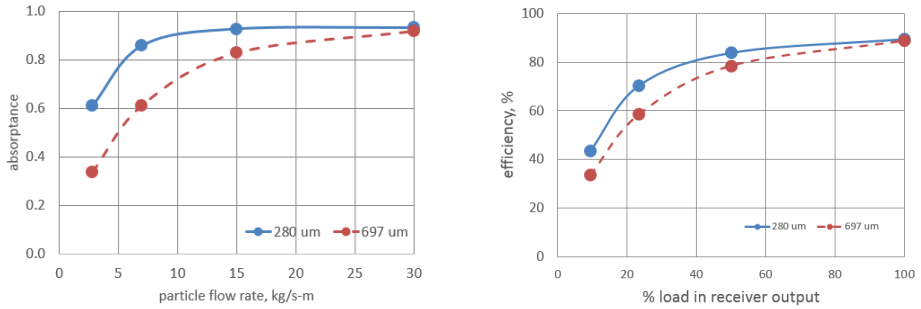

FIGURE 2. (a) Overall absorptivity of 6 m-high falling particle curtain and (b) estimated receiver efficiency.

Given the solar field and receiver geometry, the amount of solar energy provided through each cavity aperture was simulated using the Tonatiuh ray tracing software[11]. Results of the ray tracing simulation are provided in Table 3. Total energy provided at the equinox (deemed as the design condition) is 143.3 MW. This value is slightly smaller than the intended design value including energy loss, which might be related to relatively high spillage of solar energy (ranged 6.6% to 11.3%). The amount of spilt energy is expected to be reduced by further customizing the solar field suitable for the multiple cavity receiver concept, since the reference solar field was optimised for a cylindrical receiver. The maximum amount of solar energy through any one of the apertures occurs at the winter solstice for the southern cavity. If solar noon at the equinox is chosen as the design condition, the capacity of southern cavity receiver can be considered as the full load. The overall receiver efficiency will be slightly smaller than the full load efficiency (by around 1.5%), due to slight part load operations of the cavity receivers on the other sides.

TABLE 3. Spillage and solar energy provision through aperture (time: solar noon)

	Spillage, %			Energy through aperture, MW		
	summer solstice	equinox	winter solstice	summer solstice	equinox	winter solstice
East	8.6	8.8	9.0	36.1	35.6	34.0
West	8.9	9.1	9.6	36.7	36.2	34.5
South	11.3	10.9	11.1	40.2	44.8	47.4
North	6.6	8.0	11.2	31.8	26.8	20.4
Total				144.9	143.3	136.4

SOLAR EXPANDING-VORTEX RECEIVER

The development of the Solar Expanding-Vortex Receiver (SEVR) at the University of Adelaide builds upon previous work on a solar vortex reactor for reacting particles in a controlled gas environment[12]. It has been identified that existing solar vortex reactors combine advantages of directly irradiated particle reactors and cavity reactors, yet feature two main disadvantages for industrial applications. Namely, i) a particle residence time distribution which is approximately independent of particle size resulting in inefficient heating of particles, and ii) a propensity for particles to deposit onto the window, potentially causing its failure. The ASTRI SEVR concept (Fig. 3) has a number of distinctive features: it uses non-reacting particles for energy absorption and transport, and is down-facing, inclined towards the heliostat field. Its configuration differs from that of previous solar vortex receivers[13] by the following key features[14]

- particles and fluids are injected tangentially into the receiver at the opposite end of the receiver to the aperture;
- the receiver features a conical inlet expansion;
- the receiver outlets are located slightly below the plane of the aperture with a radial orientation.

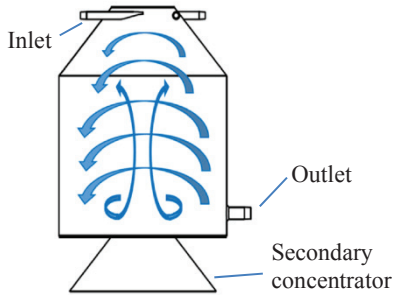

FIGURE 3. Simplified representation of the 3D flow-field within the SEVR

A joint numerical and experimental investigation of SEVR operation with a particle volume fraction, ϕ, in the range $2e^{-5}$-$5e^{-5}$ (i.e. two-way coupling regime, the particle-particle interactions are negligible) has led to the proposal of a number of mechanisms by which the SEVR addresses the above-mentioned inefficiencies of vortex receivers[12, 14].

Reduced Particle Deposition

The aerodynamic mechanisms to mitigate particle deposition onto the window are outlined as follows[12, 14, 15]

- By positioning the inlet of the receiver at the opposite end to the aperture the well-known central recirculation zone causes a pressure gradient that drives particles away from the aperture rather than towards it. It also means that the vortex intensity is significantly reduced at the plane of the aperture relative to its strength at the inlet plane, hence reducing the transport of particles through the aperture.
- The cone angle has a significant influence on both the size and strength of the vortex core. A cone angle may be chosen such that the vortex core diameter at the aperture plane is larger than the aperture, thereby mitigating particle transport through it. Furthermore, with a larger cone angle the intensity of the vortex at the aperture is reduced.

- The size of the aperture has only a minor influence on the vortex structure. Therefore, it is possible to configure the SEVR such that the aperture to receiver diameter ratio, d_{ap}/D_c, is in the range 0.125-0.375, which is optimal to mitigate particle egress through the aperture (assuming that the vortex core diameter is larger than the aperture diameter, $d_{v,max,ap}/d_{ap} > 1$).

Increased Particle Residence Time

The mechanisms to increase the particle residence time distribution of larger particles are outlined as follows[12, 14]:

- The radial outlet inhibits larger particles from leaving the reactor due to greater inertia in the vortex flow;
- The conical inlet of the receiver is able to funnel larger particles (relative to smaller particles) into the most intense part of the vortex.

Advantages

The SEVR retains all the advantages of conventional particle receivers, such as the potential to achieve higher temperatures in comparison with tubular receivers. In addition, the SEVR presents the following advantages over existing solar vortex particle receiver technologies:

- The vortex structure can be controlled by the geometric features of the receiver, thereby greatly reducing the propensity for particles to egress through the aperture and deposit onto the window. This also leads to a significant reduction of the auxiliary purging gases (less than 1% of the total inlet gas flow rate);
- The receiver can be operated potentially without the need for a window, for heating non-reacting particles, with significant benefits on the overall performance, costs and robust operation;
- A residence time distribution dependent on particle size can be achieved such that larger particles, requiring longer residence times to heat-up to a given temperature, are preferentially retained within the receiver relative to smaller particles. Therefore, a more uniform temperature distribution of the directly irradiated particles can be achieved. Also, the receiver allows for use of a wider range of particle size (as well as heterogeneous materials), hence enhancing the flexibility of this type of particle receiver;
- The SEVR can be mounted horizontally or vertically without affecting the aerodynamic features.

Disadvantages

- Particle volume fractions in a SEVR is typically in the order of 10^{-4}-10^{-5} and it requires a large amount of gas to achieve the required mass flow rate of radiation absorbing particles. In particular, the ratio of heat capacity for the solid and transport medium, where the heat capacity is defined as the mass flow rate times the specific heat, is up to 10. This, in turn, may incur higher parasitic losses (5-10% of the gross electrical output of the plant depending on the level of storage);

Performance Analysis

To make a preliminary estimate the thermal efficiency, η_{th}, of the SEVR for this paper, the radiative transfer and energy equations were included in a CFD model of the SEVR developed previously[12, 14]. A simplified approach was employed to model the concentrated solar radiation entering the cavity, applying a uniform heat flux as a boundary condition at the aperture. Note at this stage, the CFD analysis is based on a much smaller scale receiver (100kWth) than suitable for the 25 MWe ASTRI reference case, because of the availability of experimental data at this scale, and because of the computational intensity of the CFD analysis, however, a simulation of the full-scale receiver is under development. The discrete ordinates method was selected to describe the radiative equation and the particle-radiation interactions were considered in the model (including particle scattering). Air was employed as transport medium and the particle load (volume fraction) was fixed to 5 e^{-5}. Mono-sized particle injections of CARBOHSP® [16], with a particle size of 10 and 150 μm, were considered in the investigation. The calculated thermal efficiency, η_{th}, defined as the ratio of the useful heat absorbed (by particles and transport medium) and the power input, was determined in the range 0.85-0.89, depending on the particle size. In particular, for the configuration and operative conditions considered in the current study (details of the configuration investigated here can be found in Chinnici et

al.[14]), larger particles provided a larger η_{th}, due to reduced re-radiation losses through the aperture (the walls of the SEVR were considered adiabatic). Owing to the aerodynamic features of the SEVR, larger particles are preferentially retained within the receiver relative to smaller particles, and are distributed at the receiver walls and in the conical expansion rather than the vortex core and/or the aperture plane.

FLUX-OPTIMISED SODIUM RECEIVER

High thermal conductivity makes sodium an attractive heat transfer fluid for CST receivers because the good heat transfer potentially allows high solar flux, a smaller absorber area and lower thermal losses[17]. Pye et al.[18] used exergy analysis to show that sodium's high conductivity may lead to better system performance, perhaps upward of 15% higher than current state-of-the-art molten salt systems. The present work within ASTRI explores the challenges associated with high-flux operation, relating to receiver external and internal geometries, and containment materials, and presents some performance modelling results based on a simple 1D heat transfer model.

External Geometry

Development of the Flux-Optimised Sodium Receiver (FONaR) at the Australian National University (ANU) is motivated by exergy analysis showing performance gains from setting temperature distribution in a receiver in an exergetically optimal way[19]. However, practical constraints relating to containment materials, due to high tube wall stresses from combined high temperature and flux, mean that not all this benefit can be realised and a more sophisticated approach is required for setting the external geometry in receiver design. A multi-objective stochastic optimisation method has been developed integrating Monte-Carlo ray tracing and an evolutionary approach to explore promising receiver geometries and fluid paths to explore a class of sodium receiver geometries. The method is inspired from Simulation-Optimisation algorithms that are dedicated to solve "black-box" problems where it is not possible for the optimisation algorithm to reliably evaluate gradients in the model. A population of receivers is evaluated with a set of objective functions, and compared to each other using multi-dimensional Pareto dominance and considering the uncertainties due to Monte-Carlo ray tracing. The outcome of the method is a population of Pareto optimal geometries from which a design can be drawn depending on the level of performance required in each of the objectives. The method, potentially computationally intensive due to the use of Monte-Carlo ray-tracing, is greatly accelerated by using a progressive ray-tracing technique where only statistically fit candidates progress through the optimisation and under-performing candidates are discarded and not simulated further as soon as they are identified[20].

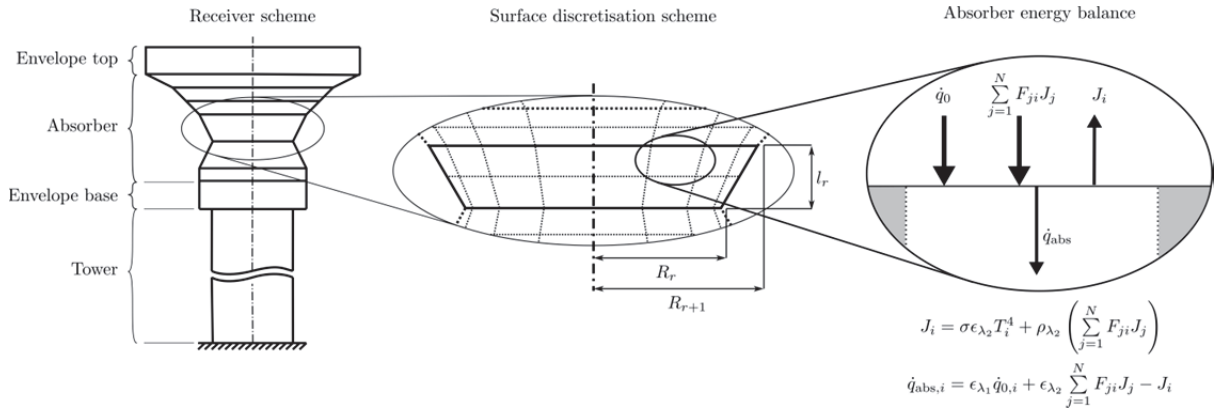

FIGURE 4. Axisymmetric receiver geometry classes considered so far for the FONaR and the corresponding discretization scheme and wall radiative heat transfer balance.

Thus far only relatively simple axisymmetric shapes have been evaluated using this method (Fig. 4). Because axisymmetric shapes with highest thermal efficiency tend to have smaller apertures, these shapes tend to suffer from more spillage which can offset some of the efficiency gains overall. Further outcomes, with more complex geometries, will be reported in future work.

Internal Geometry

A model of tube wall heat transfer for a tubular sodium receiver using a simplified two-dimensional model was developed by Logie et al.[21] in OpenFOAM, for the purpose of observing temperature and heat transfer in tubes, to compare the effect of sodium as a working fluid with molten salt. A parametric study using this model examined the dependency of internal convective heat transfer on tube diameter, mass flow and bulk fluid temperature for both fluids. It was found that the performance of sodium tubular receivers is relatively insensitive to a wide range of tube diameters and mass flows. This suggests more flexibility in the design of sodium flow conduits than is possible with molten salt.

Containment Materials

High-flux, high-temperature operation introduces challenges for containment materials in a tubular sodium receiver. Fig. 5 shows results from a case study modelling the stress in the walls of a circular pipe with sodium flow, assuming collimated heat flux. Full modelling assumptions are described in Logie et al.[21] Fig. 5a shows an example plot with solar flux at 2500 kW/m², and bulk fluid temperature at 700°C, which is the target outlet temperature for the ASTRI sodium receiver. Haynes® 230 is selected as the material for this case study as an example of a high performing alloy, with high-temperature strength and resistance to oxidizing environments. Allowable stress from the ASME Boiler and Pressure Vessel Code is plotted in Fig. 5b for Haynes® 230.

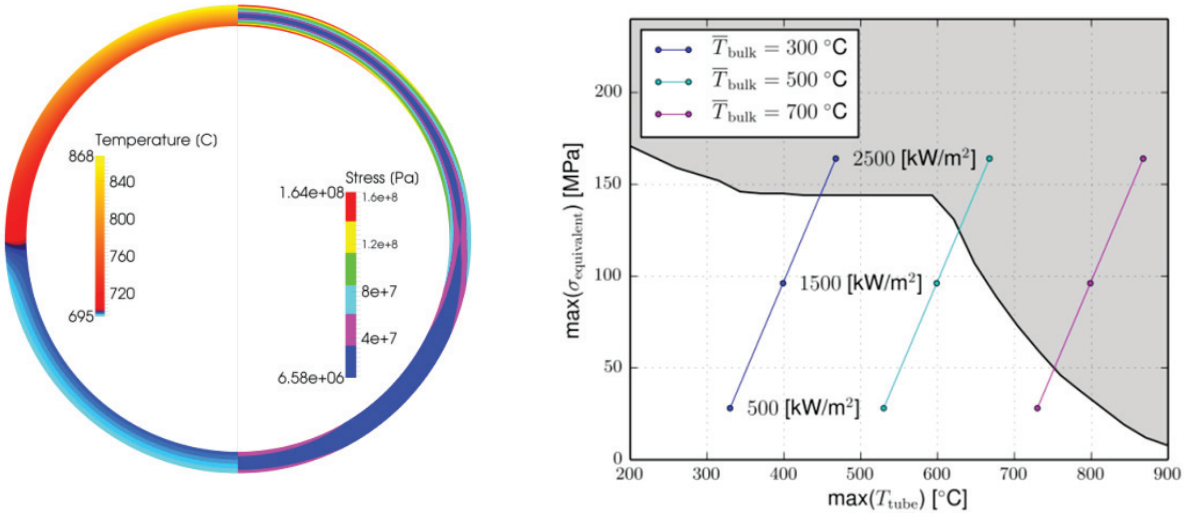

(a): Tube temperature (left) and equivalent stress (right) with a collimated heat flux of 2500 kW/m² and bulk sodium temperature 700°C

(b): Peak equivalent stress versus peak tube temperature of a range of heat fluxes and bulk sodium temperatures; unshaded region is acceptable (ASME)

FIGURE 5. Thermal stress in an exemplary length of 20 mm Haynes® 230 tube (1 mm wall thickness) using liquid sodium as a heat transfer fluid

Superimposed on Fig. 5b are three lines, each corresponding to a tube with sodium at a different bulk temperature (300°C, 500°C and 700°C). Each line shows the progression of peak equivalent stress as the solar flux intensity increases. At 700°C (the target outlet temperature for the ASTRI receiver) the tubes can withstand flux no more than 800 kW/m², whereas at 300°C, flux can be as high as 2200 kW/m². Understanding the relationship between the flux limits and bulk fluid temperature is required as an input to the design of the receiver geometry, flow path, and heliostat aiming strategy. In future work, results from stress analysis of sodium tubular receivers will constrain the multi-objective optimisation used in the development of new receiver designs, to ensure concepts are both highly performing and practically realisable with existing materials.

Performance Analysis

A sodium tubular receiver model for a cylindrical receiver has been constructed using the one-dimensional model of Pye et al[18]. The model includes external natural convection losses, radiative losses, pressure drops, wall conduction and internal convection, and assumes a uniform flux on the receiver. The outlet temperature is 700°C, with an inlet/outlet temperature difference of 138°C, dictated by the requirements of a supercritical carbon dioxide power cycle, albeit a lower temperature version than for the particle receiver system configuration. Parameters used for the study are listed in Table 4a. Assumptions about receiver size and concentration ratio are provisional, until a matched solar field model can be developed. The model results at a design-point DNI of 1000 W/m^2 are shown in Table 4b below:

TABLE 4. Parameters for (a) a scaled up sodium receiver and (b) design point specifications and performance.

(a)

Parameter		Value	Units
Concentration ratio	C	1600	
Absorbed heat	$Q_{i,tot}$	145	MWth
Outlet pressure	p_0	1	bar
Inlet temperature	T_o	562°C	°C
Outlet temperature	T_i	700°C	°C
Receiver height	L	10	m
Tube internal diameter	t	10	mm
External convection coefficient	$h_{ext,conv}$	30	W/m²

(b)

Parameter		Value	Units
Energy efficiency	η_I	87.8	%
Exergy efficiency	η_{II}	63.6	%
Inlet pressure	p_i	3.97	bar
Mass flow rate	$\dot{m}$	839	kg/s
Mass flow rate per tube	$\dot{m}_1$	0.585	kg/s
Number of tubes	n_{tubes}	1434	
Receiver width	W	17.2	m

CONCLUSIONS

Two particle receiver concepts and one sodium receiver concept were chosen for development within the ASTRI program, following an in-depth scoping study. These receiver technologies were assessed as the most likely candidates for high-efficiency performance at the elevated temperature levels required for next-generation power cycles, such as the supercritical CO_2 Brayton cycle. To date, research effort has focused on evolving the three receiver concepts, supported by heat transfer and optical modelling, understanding optical properties and durability of particles, and practical issues such as particle conveyance and deposition on windows, selection of containment materials, and investigation of other possible failure modes. Performance simulations, while preliminary, give an indication of the promise of the three technologies (Table 5).

TABLE 5. Summary of preliminary receiver efficiency modelling results

Receiver type	Receiver efficiency
Falling particle receiver	89%-90%
Solar expanding-vortex receiver	85%-89%
Flux-enhanced sodium receiver	88%

Although a coordinated approach has been taken to setting the high-level design requirements for the receivers, many of the detailed modelling assumptions are different for the performance models for the three receiver concepts, and hence the results presented in Table 5 are grouped not for direct performance comparison to each other, but rather to indicate that all three concepts show promise to achieve high efficiency. It is the intention within the ASTRI program to carry out laboratory scale testing for all three receiver concepts, leading to on-sun demonstration at the 250-500 kWth scale. It is unusual for three very different receiver designs to be compared via a coordinated approach within a single project. Through this project, ASTRI provides unique insight into the relative merits and challenges associated with these different receiver types.

ACKNOWLEDGEMENTS

This research was performed as part of the Australian Solar Thermal Research Initiative (ASTRI), a project supported by the Australian Government, through the Australian Renewable Energy Agency (ARENA).

REFERENCES

1. P. Falcone, J. Noring and J. Hruby, in *SAND85-8208* (1985).
2. N. P. Siegel, C. K. Ho, S. S. Khalsa and G. J. Kolb, Journal of Solar Energy Engineering **132** (2), 021008-021008 (2010).
3. M. Roger, L. Amsbeck, B. Gobereit and R. Buck, *Face-down solid particle receiver using recirculation*, presented at the 16th annual SolarPACES symposium, Perpignan, 2010.
4. B. Gobereit, L. Amsbeck, R. Buck, R. Pitz-Paal, M. Röger and H. Müller-Steinhagen, Solar Energy **115**, 505-517 (2015).
5. C. K. Ho, J. M. Christian, J. Yellowhair, N. Siegel, S. Jeter, M. Golob, S. I. Abdel-Khalik, C. Nguyen and H. Al-Ansary, AIP Conference Proceedings **1734** (1), 030022 (2016).
6. A. Kumar, J.-S. Kim and W. Lipinski, *Radiation absorption and temperature profiles in a particle curtain exposed to direct high-flux irradiation.* (Applied Mathematical Modelling, submitted, 2016).
7. J.-S. Kim, A. Kumar and C. Corsi, *Design Boundaries of Large-Scale Falling Particle Receivers*, presented at the 22nd SolarPACES conference, Abu Dhabi, 2016.
8. A. Kumar and J.-S. Kim, *Hydrodynamics and radiation extinction characteristics for a free falling solid particle receiver*, presented at the Eleventh International Conference on CFD in the Minerals and Process Industries, Melbourne, 2015.
9. C. K. Ho, J. Christian, D. Romano, J. Yellowhair and N. Siegel, *Characterization of Particle Flow in a Free-Falling Solar Particle Receiver*, presented at the ASME 2015 9th International Conference on Energy Sustainability, San Diego, 2015.
10. J. Kim, J.-S. Kim and W. Stein, Solar Energy **116**, 314-322 (2015).
11. Tonatiuh, release 2.2.1, http://iat-cener.github.io/tonatiuh/.
12. A. Chinnici, M. Arjomandi, Z. F. Tian, Z. Lu and G. J. Nathan, Solar Energy **122**, 58-75 (2015).
13. A. Steinfeld, Solar Energy **78** (5), 603-615 (2005).
14. A. Chinnici, M. Arjomandi, Z. F. Tian and G. J. Nathan, Solar Energy **133**, 451-464 (2016).
15. A. Chinnici, Y. Xue, T. C. W. Lau, M. Arjomandi and G. J. Nathan, Solar Energy **141**, 25-37 (2017).
16. N. Siegel, M. Gross and C. Ho, *Physical Properties of Solid Particle Thermal Energy Storage Media for Concentrating Solar Power Applications*, presented at the SolarPACES 2013, 2013.
17. J. Coventry, C. Andraka, J. Pye, M. Blanco and J. Fisher, Solar Energy **122**, 749-762 (2015).
18. J. Pye, M. Zheng, C.-A. Asselineau and J. Coventry, *An exergy analysis of tubular solar-thermal receivers with different working fluids*, presented at the 20th annual SolarPACES symposium, Beijing, 2014.
19. C.-A. Asselineau and J. Pye, *Exergetic efficiency of point-focus concentrators under realistic angular radiation distributions*, presented at the Asia-Pacific Solar Research Conference, Brisbane, 2015.
20. C.-A. Asselineau, J. Zapata and J. Pye, Optics Express **23** (11), A437-A443 (2015).
21. W. Logie, C.-A. Asselineau, J. Pye and J. Coventry, *Temperature and Heat Flux Distributions in Sodium Receiver Tubes*, presented at the Asia-Pacific Solar Research Conference, Brisbane, 2015.